European Journal of Applied Physiology
https://doi.org/10.1007/s00421-018-3798-y

ORIGINAL ARTICLE

Passive stiffness of monoarticular lower leg muscles is influenced by knee joint angle

Filiz Ateş[1,2] · Ricardo J. Andrade[1,3] · Sandro R. Freitas[3,4] · François Hug[1,5,6] · Lilian Lacourpaille[1] · Raphael Gross[1,7] · Can A. Yucesoy[2] · Antoine Nordez[1,8]

Received: 9 May 2017 / Accepted: 24 December 2017
© Springer-Verlag GmbH Germany, part of Springer Nature 2018

Abstract

Purpose While several studies demonstrated the occurrence of intermuscular mechanical interactions, the physiological significance of these interactions remains a matter of debate. The purpose of this study was to quantify the localized changes in the shear modulus of the gastrocnemius lateralis (GL), monoarticular dorsi- and plantar-flexor muscles induced by a change in knee angle.

Method Participants underwent slow passive ankle rotations at the following two knee positions: knee flexed at 90° and knee fully extended. Ultrasound shear wave elastography was used to assess the muscle shear modulus of the GL, soleus [both proximally (SOL-proximal) and distally (SOL distal)], peroneus longus (PERL), and tibialis anterior (TA). This was performed during two experimental sessions (experiment I: $n = 11$; experiment II: $n = 10$). The shear modulus of each muscle was compared between the two knee positions.

Results The shear modulus was significantly higher when the knee was fully extended than when the knee was flexed ($P < 0.001$) for the GL (averaged increase on the whole range of motion: $+5.8 \pm 1.3$ kPa), SOL distal ($+4.5 \pm 1.5$ kPa), PERL ($+1.1 \pm 0.7$ kPa), and TA ($+1.6 \pm 1.0$ kPa). In contrast, a lower SOL-proximal shear modulus ($P < 0.001$, -5.9 ± 1.0 kPa) was observed.

Conclusion As the muscle shear modulus is linearly related to passive muscle force, these results provide evidence of a non-negligible intermuscular mechanical interaction between the human lower leg muscles during passive ankle rotations. The role of these interactions in the production of coordinated movements requires further investigation.

Keywords Ultrasound · Shear modulus · Shear wave elastography · Intermuscular mechanical interactions · Epimuscular myofascial force transmission

Abbreviations

ANOVA	Analysis of variance
EMG	Electromyography
GL	Gastrocnemius lateralis
GM	Gastrocnemius medialis

Communicated by Olivier Seynnes.

Filiz Ates and Ricardo J. Andrade contributed equally to this work.

✉ Antoine Nordez
antoine.nordez@univ-nantes.fr

[1] Laboratory "Movement, Interactions, Performance" (EA 4334), Faculty of Sport Sciences, Université de Nantes, UFR STAPS, 25 bis Bd Guy Mollet, BP 72206, 44000 Nantes, France

[2] Institute of Biomedical Engineering, Bogazici University, Istanbul, Turkey

[3] Universidade de Lisboa, Faculdade de Motricidade Humana, Estrada da Costa, Cruz Quebrada-Dafundo, 1499-002 Lisbon, Portugal

[4] Benfica Lab, Sport Lisboa e Benfica, Lisbon, Portugal

[5] NHMRC Centre of Clinical Research Excellence in Spinal Pain, Injury and Health, School of Health and Rehabilitation Sciences, The University of Queensland, Brisbane, Australia

[6] Institut Universitaire de France (IUF), Paris, France

[7] Gait Analysis Laboratory, Physical and Rehabilitation Medicine Department, University Hospital of Nantes, Nantes, France

[8] Health and Rehabilitation Research Institute, Faculty of Health and Environmental Sciences, Auckland University of Technology, Auckland, New Zealand

Published online: 11 January 2018

MRI	Magnetic resonance imaging
PERL	Peroneus longus
ROI	Region of interest
ROM	Range of motion
SOL	Soleus
SSI	Supersonic shear imaging
TA	Tibialis anterior

Introduction

Muscle–tendon units are commonly considered as independent actuators (e.g., Zajac 1989; Buchanan et al. 2004). However, intermuscular mechanical interactions are plausible through at least two mechanisms. The first is the myofascial force transmission mechanism (Huijing 2009; Yucesoy 2010). Intramuscular connective tissues are attached to muscle fibers along their full length (Berthier and Blaineau 1997), allowing for muscle fiber–endomysium interactions (Street 1983). This can lead to lateral muscle force transmission from the muscle fibers onto the extracellular matrix, called intramuscular myofascial force transmission (Huijing 1999). In addition, collagen reinforced fascial structures (e.g., neurovascular tracts) interconnect adjacent muscles and can also provide connections between distant muscles (Huijing 2009). Such intra- and intermuscular myofascial force transmission pathways are continuous, and in combination, they are referred to as epimuscular myofascial force transmission (Huijing 2009). The second is via the shared tendon if two different muscles are connected to the same tendon such as the Achilles tendon.

Evidence of intermuscular mechanical interactions was demonstrated in animal experiments that reported different force levels between the proximal and the distal tendons of a muscle (Huijing and Baan 2001; Maas et al. 2001; Yucesoy et al. 2006). In addition, while altering the length of a muscle–tendon unit experimentally, some studies observed a change in force of neighbouring muscles despite their length remained unchanged (Huijing et al. 2007; Maas et al. 2005). However, the physiological significance of these interactions remains a matter of debate. A series of recent studies showed that they are negligible in rat ankle plantar flexors (Tijs et al. 2015, 2016a) and anterior crural compartment (Tijs et al. 2016b).

In humans, Bojsen-Moller et al. (2010) showed that changes in knee angle affect soleus (SOL) fiber length measured using ultrasound, although this muscle does not cross the knee joint. This provides indirect evidence that mechanical interactions occur between the SOL and neighbouring structures that cross the knee joint such as the gastrocnemii muscles, which was further confirmed by Huijing et al. (2011) using magnetic resonance imaging (MRI). Similar protocols reported substantial local strains along medial gastrocnemius muscle fibers (Pamuk et al. 2016; Karakuzu et al. 2017) and also within other lower leg monoarticular muscles such as deep flexor, anterior crural, and peroneal muscle groups (Yaman et al. 2013). However, the physiological significance of intermuscular mechanical interactions remains unknown and is challenging to assess in vivo in human. Indeed, due to non-linear force–length relationships of biological tissues, large displacements occur at low force levels. Therefore, the magnitude of transmitted force cannot be inferred from muscle displacements measured using imaging modalities including B-mode ultrasound and MRI.

Supersonic shear imaging (SSI) is an ultrasound shear wave elastography technique that estimates the shear modulus of soft tissues (Bercoff et al. 2004). Muscle shear modulus measured with this technique provides an accurate measurement of localized muscle stiffness (Eby et al. 2013) and is strongly linearly related to both active and passive muscle force (for a review see Hug et al. 2015). Therefore, a change in muscle shear modulus can be directly interpreted as a change in muscle force. As such, SSI provides a unique opportunity to provide a more direct evidence of intermuscular mechanical interactions in humans.

The aim of the present study was to measure the shear modulus of lower leg muscles during passive ankle rotations performed with the knee flexed at 90° and fully extended. The changes in knee angle should alter the gastrocnemii muscle length independently of other lower leg muscles that do not cross the knee. Considering that intermuscular mechanical interactions occur between the gastrocnemius and monoarticular leg muscles, we hypothesized that knee extension induces a concomitant increase in the shear modulus of gastrocnemii muscle and both monoarticular plantar flexors [soleus (SOL) and peroneus longus (PERL)] and dorsiflexors [tibialis anterior (TA)]. These muscles were studied in two separate experiments: experiment I—SOL (proximal and distal parts) and gastrocnemius lateralis (GL) and experiment II—TA, PERL, and GL. The lower leg muscles were chosen as: (1) they have a crucial role in human locomotion; (2) they provide the opportunity to assess force transmission between mono and biarticular muscles that share a common tendon (experiment 1) and muscles that do not share any tendon (experiment 2); and (3) the ease of use of the elastography technique on these muscles.

Materials and methods

Participants

Eleven healthy participants were involved in Experiment I (10 males and 1 female; age: 26.9 ± 2.2 years, height: 179.3 ± 8.7 cm, weight: 72.4 ± 5.8 kg), and ten other healthy participants were involved in Experiment II (5 males and

5 females; age: 24.6 ± 2.2 years, height: 172.1 ± 4.4 cm, weight: 69.9 ± 7.5 kg). The participants were informed about the purpose of the study and methods used before providing informed consent. The Local Ethics Committee approved the study, and all procedures conformed to the Declaration of Helsinki.

Measurements

Ergometer

For both experiments, an isokinetic dynamometer (Con-Trex MJ; CMV AG, Dubendorf, Switzerland) was used to measure the ankle angle during ankle rotations. The neutral position of the ankle (0°) was defined as an angle of 90° between the footplate and the shank. The lateral malleolus of the ankle joint was aligned with the rotation axis of the dynamometer.

Elastography

An Aixplorer ultrasound scanner (version 6.1; Supersonic Imagine, Aix-en-Provence, France) coupled with a linear transducer array (4–15 MHz, SL15-4, Aix-en-Provence, France) was used in Shear Wave Elastography mode (musculoskeletal preset). Assuming a linear elastic behaviour (Bercoff et al. 2004; Gennisson et al. 2003), the muscle shear modulus was calculated as follows:

$$\mu = \rho V_s^2, \quad (1)$$

where ρ is the density of muscle (1000 kg/m^3), and V_s is the shear wave velocity. The optimal transducer locations were marked on the skin using a waterproof marker to guide repeated placement throughout the trials. The ultrasound transducer was orientated parallel to the estimated muscle shortening direction (i.e., origin–insertion direction) to measure the shear modulus along the stretching direction of the muscle, as done on isolated muscles with the conventional material testing that remains the gold standard for muscle mechanical properties assessment (e.g., Eby et al. 2013). The maps of the shear modulus were visualized in real time at 1 Hz with a spatial resolution of 1 × 1 mm. Clips were saved for further analysis. For synchronization purpose, a trigger signal originating from the ultrasound scanner at each elastography measurement was recorded along with the ankle angle and torque. Since shear modulus measurements last less than 50 ms (Bercoff et al. 2004), they can be considered as instantaneous. Note that several studies reported the very good-to-excellent reliability of the measurements performed within similar experimental conditions (Lacourpaille et al. 2012; Maisetti et al. 2012; Le Sant et al. 2017). Coefficient of variations obtained for intra session reliability was consistently lower than 10%.

Protocol

The effect of knee angle on shear modulus was assessed on (1) GL and SOL muscles (Experiment I) and (2) GL, PERL, and TA muscles (Experiment II). For both experiments, the participants were previously instructed to not perform vigorous exercise in the 48 h prior to testing. The participants were blindfolded to ensure no visual perception of stretching during testing. They were instructed to stay as relaxed as possible during each trial.

Experiment I: passive dorsiflexions

The participants were positioned prone, such that ultrasound measurements could be easily performed on the posterior compartment of the leg. The hip was fixed at 0° in both the frontal and sagittal planes. Two knee angles (0°—knee fully extended and 90°—knee flexed) were tested in random order and interspaced by 5 min of rest. The shank was in the same position for both knee angles, parallel to the ergometer seat (Hoang et al. 2005). To precondition the muscles, five passive loading and unloading cycles were applied to the ankle from 40° of plantar flexion to 20° of dorsiflexion (at 5° s^{-1}). Then, actual passive cycles were performed for the same ankle range of motion (ROM) at 2° s^{-1}. The shear modulus measurements were performed in random order on the GL (muscle belly) and on two regions of the SOL (proximal: at the same probe location used for the GL; distal: lateral side of the lower leg and proximal to the Achilles tendon) (Fig. 1). Three ankle rotation cycles were performed to measure each muscle once.

Experiment II: passive plantar flexions

The participants were positioned supine, such that ultrasound measurements could be easily performed on the anterior compartment of the leg. The shank was positioned horizontally for all tests using an inclinometer. The two knee angles (0°—knee fully extended and 90°—knee flexed) were tested in random order and interspaced by 5 min of rest. For the knee-flexed position, the hip was flexed to ~ 90° (thigh perpendicular to the shank). Participants performed five passive loading and unloading ankle cycles for conditioning (5° s^{-1}) between 20° of dorsiflexion to 40° of plantar flexion. Then, actual passive cycles were performed for the same ankle ROM at 2° s^{-1}. The shear modulus measurements were performed on the PERL, TA, and GL in random order (Fig. 1). Three ankle rotation cycles were performed, such that each muscle was measured once.

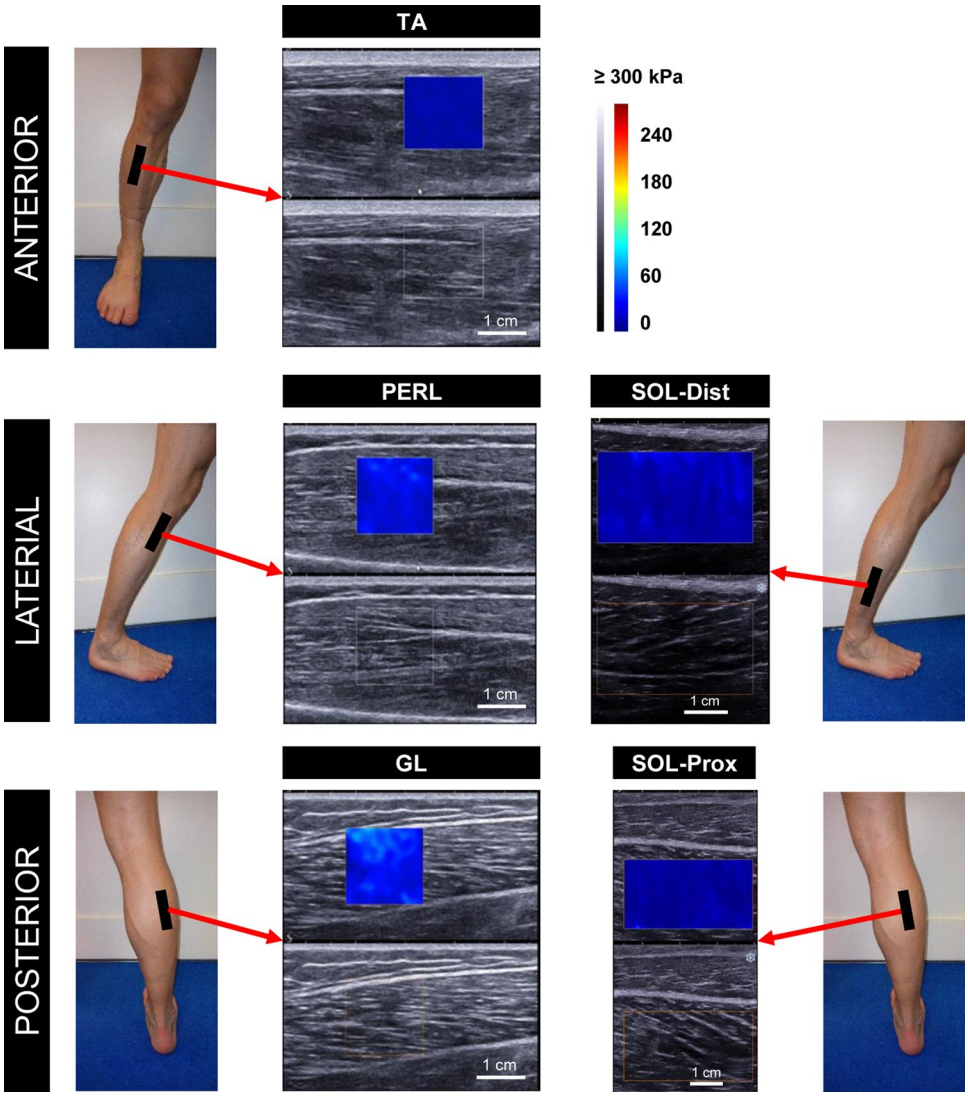


Fig. 1 Acquisition of the maps of shear modulus: muscles' probe location to the elastographic assessments. Anterior, lateral, and posterior views are depicted. *TA* tibialis anterior, *PERL* peroneus longus, *SOL-distal* distal part of Soleus, *SOL-proximal* proximal part of Soleus, *GL* gastrocnemius lateralis. (Color figure online)

Data analysis and statistics

For both experiments, the B-mode images and superposed shear modulus color maps were exported in "mp4" format and sequenced into images ("jpeg" compression). Data processing was performed using MATLAB scripts (MathWorks, Natick, USA). Image processing converted each pixel of the color map into a value of the shear modulus based on the recorded color scale. A rectangular area as large as possible, with exclusion of aponeurosis, was chosen as the region of interest (ROI) from the maps. An average value of the shear modulus over the ROI was calculated for each image and synchronized with the corresponding ankle angle using the ultrasound trigger signal. The mean ROI size (± standard deviation) was 2.14 ± 0.61, 2.27 ± 0.60, 2.10 ± 0.61, 1.54 ± 0.43, and 1.62 ± 0.39 cm^2 for GL, SOL proximal, SOL distal, PL, and TA, respectively.

In both experiments I and II, the shank was maintained in the same position for both knee angles. This was carefully checked using an inclinometer in experiment II, and using the ergometer seat in experiment I. To confirm that the ankle angle measurement did influence our findings, we performed a pilot study with four subjects, where ankle angle was measured using 3D motion analysis for both knee angles in the same conditions as in the actual experiments. We found good agreement between ankle angle measurements performed using 3D motion analysis and that performed using the ergometer for both knee angles, without significant bias (mean error of ~ 1°). It allowed us to consider that the measurement of ankle angle made by the ergometer was accurate.

MATLAB scripts were used for the statistical procedures. Distributions consistently passed the Kolmogorov–Smirnov normality test. Separate two-way analysis of variances (ANOVAs) with repeated measures [factors:

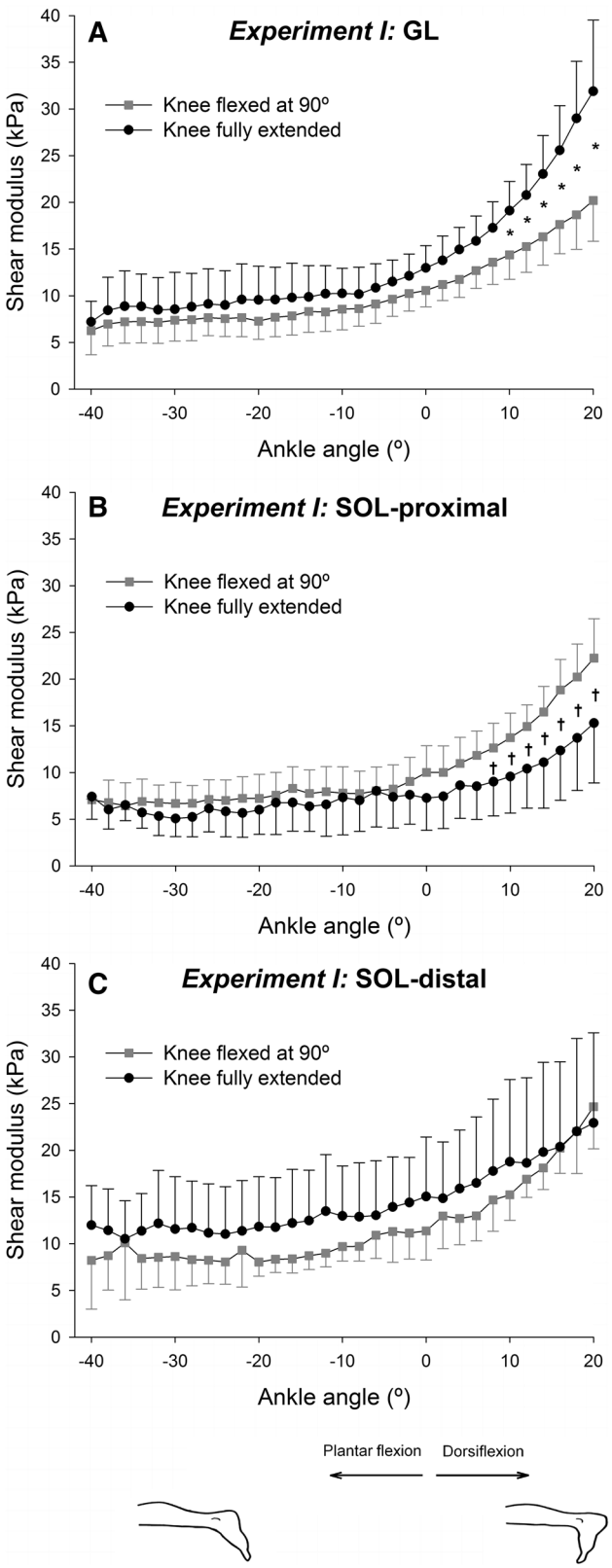


Fig. 2 Experiment I: averaged relationships between ankle angle and shear modulus for the Knee flexed at 90° and Knee fully extended by muscle: **A** gastrocnemius lateralis; **B** proximal part of Soleus (SOL-proximal); and **C** distal part of Soleus (SOL-distal). Asterisk: the shear modulus of GL (Graphic A) was significantly higher for knee fully extended vs knee flexed at 90°, between 10 and 20°: P values <0.01 for all ankle angles. Dagger: the shear modulus of SOL proximal (Graphic B) was significantly greater for knee flexed at 90° vs knee fully extended, between 8 and 20°: p values <0.01 for all ankle angles

ankle angles (from 40° of plantar flexion to 20° of dorsiflexion every 2°—31 data points in total) and knee angles (90° and 0°)] were used to analyze the effects of knee angle on shear modulus values for each muscle (experiment I: GL, SOL proximal, and SOL distal; experiment II: GL, PERL, and TA). If significant effects were found, post-hoc tests were performed using a Bonferroni correction for multiple comparisons (i.e., the level of significance was set at 0.05 divided by the number of conditions). The statistical significance was set at $P<0.05$.

Results

Experiment I

Significant main effects of ankle angle ($P<0.001$), knee angle ($P<0.001$), and an interaction between ankle and knee angles ($P<0.001$) were found for GL shear modulus. Post-hoc tests showed a significant increase in GL shear modulus at a knee angle of 0° compared to a knee angle of 90° between 10° and 20° of dorsiflexion (average increase: $+5.8\pm1.3$ kPa; $P<0.01$ for all of the angles) (Fig. 2A). The highest difference between both knee angles was 11.7 ± 7.8 kPa and it was observed at 20° of dorsiflexion.

For the SOL proximal muscle, a significant main effect of both ankle angle ($P<0.001$) and knee angle ($P<0.001$) was found. In addition, there was a significant interaction between ankle angle and knee angle ($P=0.0035$). The shear modulus of SOL proximal muscle was lower at 0° than 90° of knee angle between 8° and 20° of dorsiflexion (average decrease: -5.9 ± 1.0 kPa; $P<0.01$ for all angles) (Fig. 2B). The highest difference between both knee angles was 7.0 ± 6.9 kPa and it was observed at 20° of dorsiflexion.

For the SOL distal muscle, a significant main effect ($P<0.001$) of both ankle and knee angles ($P<0.001$) was found. However, no significant interaction ($P=0.67$) between ankle angle and knee angle was shown. In contrast to what was observed for the SOL proximal muscle, the SOL-distal shear modulus was higher at a knee angle of 0° regardless of the ankle angle (average increase on the whole range of motion: $+4.5\pm1.5$ kPa) (Fig. 2C). Note that data of two participants were not processed for this analysis because artefacts (small regions of saturated values) appeared within the shear modulus maps for this specific probe location.

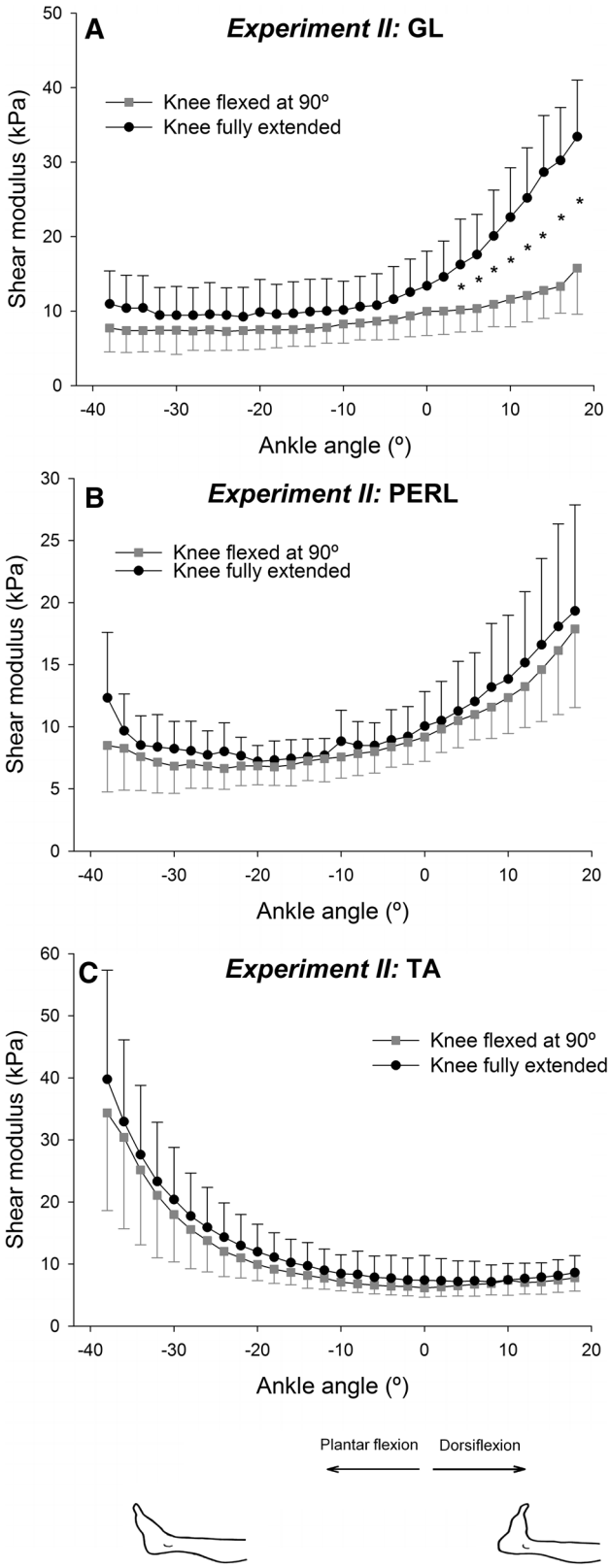


Fig. 3 Experiment II: averaged relationships between ankle angle and shear modulus for the Knee flexed to 90° and Knee fully extended by muscle: **A** gastrocnemius lateralis (GL); **B** peroneus longus (PERL); and **C** tibialis anterior (TA). Asterisk: the shear modulus of GL (Graphic A) was significantly greater for knee fully extended vs knee flexed at 90°, between 4 and 20°: *P* values < 0.01 for all ankle angles

Experiment II

For the GL muscle shear modulus, a significant main effect ($P < 0.001$) of both ankle angle and knee angle was observed. In addition, there was an interaction ($P < 0.001$) between ankle angle and knee angle. The GL shear modulus was significantly higher within the range 4°–20° of dorsiflexion when the knee was at 0° compared to when the knee was at 90° (average increase: $+12.1 \pm 4.5$ kPa ; $P < 0.01$ for all angles; Fig. 3A). The highest difference between both knee angles was 17.6 ± 7.2 kPa and it was observed at 20° of dorsiflexion.

For both the TA and PERL muscles (Fig. 3B and C), a significant main effect of ankle angle ($P < 0.001$ for both muscles) and knee angle (TA: $P = 0.0011$; PERL: $P < 0.001$) was found. However, the interaction was not significant (TA: $P = 0.99$; PERL: $P = 0.99$). The significant main effect of knee angle showed a higher mean shear modulus at a knee angle of 0° for both muscles (average increase on the whole range of motion: $+1.6 \pm 1.0$ kPa for the TA; $+1.1 \pm 0.7$ kPa for the PERL).

Discussion

The results of the present study showed that shear modulus (an index of changes in muscle force) of TA, SOL distal, and PERL was higher with the knee extended compared to the knee-flexed position, while it was lower for the SOL proximal. Therefore, our hypothesis was partly validated, and because none of these muscles crosses the knee joint, the observed change in shear modulus provides strong evidence of intermuscular mechanical interactions.

In both experiments I and II, we report an exponential increase in GL shear modulus during passive dorsiflexion. As expected, the GL shear modulus was significantly higher when the knee was fully extended than when the knee was flexed at 90° (i.e., approximately 60% of increase). This was already observed for the gastrocnemius medialis (GM) muscle (Maïsetti et al. 2012). It is important to note that the magnitude of the changes in GL shear modulus induced by the change in knee angle was lower than that of the GM, as reported by Maïsetti et al. [i.e., ~ 600% of increase at 20° of ankle angle dorsiflexion (see Fig. 2B in 2012)]. Together with other results showing that GM shear modulus is higher than the GL shear modulus (Le Sant et al. 2017; Hirata et al. 2016), this suggests that GL and GM exhibit different passive mechanical behaviours during passive stretching. This is particularly important, because GL and GM muscles are

classically pooled within the same unit (Nordez et al. 2010; Hoang et al. 2005; McNair et al. 2001).

The results observed for both the proximal and distal SOL regions highlight complex behaviour. Although the shear modulus of SOL proximal was lower when the knee was extended than when the knee was flexed, opposite behaviour was observed for SOL distal regardless of the ankle angle. As changes in the shear modulus are linearly related to the local changes in passive tension (Koo et al. 2013; Maisetti et al. 2012), these results strongly suggest that passive tension increased within SOL distal, while it decreased within SOL proximal. This might be the consequence of intermuscular mechanical interactions that would occur through two possible mechanisms. First, the knee extension would increase the length of the gastrocnemii proximally. This would cause its relative position with SOL to change, and this would lead to a proximally directed passive myofascial tension acting on SOL via stretching of the epimuscular connections (Huijing 2009). Such load can cause local unloading of SOL proximal. Similarly, it can cause tensioning of SOL distal, as observed herein. This is in agreement with our results, in particular with the observed increase in shear modulus of SOL distal. Second, the gastrocnemii and SOL are connected towards the Achilles tendon, and passive tension could be transmitted to SOL within its distal region via the tendon. However, knee extension should induce an increase in tension in the Achilles tendon, and thus a decrease in passive tension in the SOL distal (Tian et al. 2012). Therefore, since an increase in shear modulus in the SOL distal was found, this pathway remains less probable than epimuscular myofascial force transmission.

These proximo-distal differences in shear modulus of SOL suggest that intermuscular mechanical interactions are not homogeneous, and this might be due to the non-linear and complex mechanical properties of epimuscular connections. In particular, our results are consistent with local deformation heterogeneity previously reported by modelling studies and attributed to extracellular matrix–muscle fiber mechanical interactions (Yucesoy et al. 2008). Such deformation heterogeneity has also been shown in vivo in human muscles using MRI during joint movement (Huijing et al. 2011; Yaman et al. 2013). These studies demonstrated local muscle tissue lengthening and shortening occurring simultaneously within the lower leg muscles.

Assuming a linear relationship between muscle shear modulus and passive muscle tension (Hug et al. 2015; Koo et al. 2013; Maisetti et al. 2012), the results of the present study can provide an estimate of the amount of passive muscle tension transmitted to SOL. Using previously published data obtained for similar subjects (Nordez and Hug 2010), we estimated the passive tension in SOL muscle. To do so, we considered that the passive torque of monoarticular structures during ankle dorsiflexion is only attributed to SOL. Thanks to the Hoang's model (Nordez et al. 2010; Hoang et al. 2005), we estimated this torque to be ~4 N m at 20° of dorsiflexion. Considering a moment arm of approximating 4 cm (Maganaris 2004), the passive tension of SOL would be approximately 100 N. As the changes in SOL shear modulus reported in the present study at 20° of dorsiflexion ranged between +20 and +46%, it suggests that localized tension can vary between 20 and 46 N. Although our results do not demonstrate directly that mechanical interactions between SOL and gastrocnemii are physiologically relevant, it suggests that it is probably not negligible. This is strengthened by the non-homogeneous effects revealed within the SOL. Non-homogeneous effects may also explain the difference between the results of the present study, obtained with localized measurements on two distant locations, and the tension estimated by Tian et al. (2012) that was representative of the whole SOL muscle. Considering the decrease in shear modulus distal and the increase in shear modulus proximal, our results also indicate that the magnitude of the global changes in SOL tension could be low. However, the amount of localized changes remains important for the muscle that should see large localized changes in stress. Furthermore, Finni et al. (2017) have reported a different behaviour of fiber lengths between SOL distal and SOL proximal during passive knee flexion (ankle joint positioned neutral). Although these differences were not significant, the non-homogenous behaviour is in accordance with the results of the present study.

Shear modulus of TA and PERL muscles increased significantly during knee extension. While the magnitude of these changes muscles was lower than for the SOL muscle, this highlights the probable presence of significant mechanical interactions between muscles acting on the knee (e.g., gastrocnemii or hamstrings) and the distant TA and/or PERL. Since no common tendons are shared between these muscles, this result demonstrates the occurrence of epimuscular myofascial force transmission in the lower leg. Such interactions between antagonist muscles have been already reported in animal experiments (Meijer et al. 2007; Rijkelijkhuizen et al. 2007). For example, Rijkelijkhuizen et al. (2007) measured a—16% decrease in force produced by the triceps surae muscle group in rats due to lengthening of antagonist muscles (TA and extensor hallicus longus). Anatomically, the crural fascia that covers the gastrocnemii and SOL also provides an attachment, by its deep surface, to the antagonistic TA and extensor digitorum longus muscles. In addition, this fascia covers the head and malleolus of the fibula, and two strong intermuscular septa that enclose the PERL and peroneus brevis muscles emerge on the lateral side from the deep surface (Stecco and Hammer 2015; Standring 2016). More proximally, the iliotibial tract and the biceps femoris, both crossing the knee, laterally reinforce the crural fascia by providing several myofascial expansions. Such expansions

attach to the lateral condyle of the tibia and the head of the fibula, contributing to the stretch the crural fascia in both proximo-distal and latero-medial direction by the anterior knee retinaculum (Stecco and Hammer 2015). Therefore, the fascial expansions to the crural fascia would strengthen the linkage between the thigh and leg through the knee joint. Finally, the neuromuscular tract of the sciatic nerve links TA and GL and crosses the knee joint. Therefore, both fascia and nerves create robust epimuscular connections between the GL, TA, PERL, and SOL muscles. This might explain the changes in shear modulus that we observed due to change in knee angle.

One limitation of our study is that we did not evaluate the myoelectric activity to ensure that the muscles remained passive. However, each participant was verbally instructed to stay relaxed before each passive ankle rotation. In addition, B-mode ultrasound images and passive torque were recorded and visually inspected. Thus, any muscle contraction would have been detected in the B-mode images and torque–angle data (Tian et al. 2012). We cannot roll out the effect of a slight muscle activation on the observed changes in shear modulus. However, similar experiments performed in healthy young adults reported systematic low EMG amplitude values (< 1% of maximal EMG amplitude) during submaximal stretch as performed herein (Andrade et al. 2016; McNair et al. 2001), further suggesting that healthy young participants can remain fully relaxed during slow movements.

Conclusions

Taking advantage of shear wave elastography, the present study strongly suggests that intermuscular mechanical interactions occur in passive human muscles of the lower leg. These interactions can occur both between adjacent synergist muscles (e.g., SOL and GL; SOL and PERL) and between antagonist muscles (e.g., TA and GL), suggesting that various pathways may be involved. In addition, our results demonstrate opposite changes in shear modulus within two SOL regions due to gastrocnemius tensioning, indicating that these interactions are region-dependant. This highlights the need for localized measurements, such as shear wave elastography, to better understand the physiological relevance of intermuscular mechanical interactions in healthy and pathological muscles. As the previous studies suggested different contributions of these interactions during contraction and passive stretching (Bojsen-Moller et al. 2010; Finni et al. 2017), it is important to analyze these interactions during various tasks using elastography. In addition, they are thought to play an important role in people with neurological conditions (Ates et al. 2014). Further research is thus needed to determine the functional impact of intermuscular mechanical interactions on movement in health and disease.

Acknowledgements This study was supported by grants from the European Regional development Fund (ERDF, no. 37400), the Region Pays de la Loire (QUETE project), and by the Interdisciplinary program from the University of Nantes.

Author contributions FA, RJA, SRF, CAY, RG, FH, and AN conceived and designed research. FA, RJA, SRF, and LL conducted experiments. FA, RJA and AN analyzed data. FA and RJA wrote the manuscript. All authors read and approved the manuscript.

Compliance with ethical standards

Conflict of interest The authors have no conflict of interest.

References

Andrade RJ, Lacourpaille L, Freitas SR, McNair PJ, Nordez A (2016) Effects of hip and head position on ankle range of motion, ankle passive torque, and passive gastrocnemius tension. Scand J Med Sci Sports 26(1):41–47

Ates F, Temelli Y, Yucesoy CA (2014) Intrapoerative experiments show relevance of inter-antagonistic mechanical interaction for spastic muscle's contribution to joint movement disorder. Clin Biomech 29(8):943–949

Bercoff J, Tanter M, Fink M (2004) Supersonic shear imaging: a new technique for soft tissue elasticity mapping. IEEE Trans Ultrason Ferroelectr Freq Control 51(4):396–409

Berthier C, Blaineau S (1997) Supramolecular organization of the subsarcolemmal cytoskeleton of adult skeletal muscle fibers. A review. Biol Cell 89(7):413–434

Bojsen-Moller J, Schwartz S, Kalliokoski KK, Finni T, Magnusson SP (2010) Intermuscular force transmission between human plantarflexor muscles in vivo. J Appl Physiol 109(6):1608–1618

Buchanan TS, Lloyd DG, Manal K, Besier TF (2004) Neuromusculoskeletal modeling: estimation of muscle forces and joint moments ans movements from measurements of neural command. J Appl Biomech 20(4):367–395

Eby SF, Song P, Chen S, Chen Q, Greenleaf JF, An KN (2013) Validation of shear wave elastography in skeletal muscle. J Biomech 46(14):2381–2387

Finni T, Cronin NJ, Mayfield D, Lichtwark GA, Cresswell AG (2017) Effects of muscle activation on shear between human soleus and gastrocnemius muscles. Scand J Med Sci Sports 27(1):26–34

Gennisson JL, Catheline S, Chaffai S, Fink M (2003) Transient elastography in anisotropic medium: application to the measurement of slow and fast shear wave speeds in muscles. J Acoust Soc Am 114(1):536–541

Hirata K, Miyamoto-Mikami E, Kanehisa H, Miyamoto N (2016) Muscle-specific acute changes in passive stiffness of human triceps surae after stretching. Eur J Appl Physiol 116(5):911–918

Hoang PD, Gorman RB, Todd G, Gandevia SC, Herbert RD (2005) A new method for measuring passive length-tension properties of human gastrocnemius muscle in vivo. J Biomech 38(6):1333–1341

Hug F, Tucker K, Gennisson JL, Tanter M, Nordez A (2015) Elastography for muscle biomechanics: toward the estimation of individual muscle force. Exerc Sport Sci Rev 43(3):125–133

Huijing P (1999) Muscular force transmission: a unified, dual or multiple system? A review and some explorative experimental results. Arch Physiol Biochem 107(4):292–311

Huijing PA (2009) Epimuscular myofascial force transmission: a historical review and implications for new research. International Society of Biomechanics Muybridge Award Lecture, Taipei, 2007. J Biomech 42(1):9–21

Huijing PA, Baan GC (2001) Extramuscular myofascial force transmission within the rat anterior distal compartment: proximo-distal differences in muscle force. Acta Physiol Scand 173(3):297–311

Huijing PA, van de Langenberg RW, Meesters JJ, Baan GC (2007) Extramuscular myofascial force transmission also occurs between synergistic muscles and antagonistic muscles. J Electromyogr Kinesiol 17(6):680–689. https://doi.org/10.1016/j.jelekin.2007.02.005

Huijing PA, Yaman A, Ozturk C, Yucesoy CA (2011) Effects of knee joint angle on global and local strains within human triceps surae muscle: MRI analysis indicating in vivo myofascial force transmission between synergistic muscles. Surg Radiol Anat 33(10):869–879

Karakuzu A, Pamuk U, Ozturk C, Acar B, Yucesoy CA (2017) Magnetic resonance and diffusion tensor imaging analyses indicate heterogeneous strains along human medial gastrocnemius fascicles caused by submaximal plantar-flexion activity. J Biomech 57:69–78

Koo TK, Guo JY, Cohen JH, Parker KJ (2013) Relationship between shear elastic modulus and passive muscle force: an ex-vivo study. J Biomech 46(12):2053–2059. https://doi.org/10.1016/j.jbiomech.2013.05.016

Lacourpaille L, Hug F, Bouillard K, Hogrel JY, Nordez A (2012) Supersonic shear imaging provides a reliable measurement of resting muscle shear elastic modulus. Physiol Meas 33(3):N19–N28. https://doi.org/10.1088/0967-3334/33/3/N19

Le Sant G, Nordez A, Andrade R, Hug F, Freitas S, Gross R (2017) Stiffness mapping of lower leg muscles during passive dorsiflexion. J Anat 230(5):639–650

Maas H, Baan GC, Huijing PA (2001) Intermuscular interaction via myofascial force transmission: effects of tibialis anterior and extensor hallucis longus length on force transmission from rat extensor digitorum longus muscle. J Biomech 34(7):927–940

Maas H, Meijer HJ, Huijing PA (2005) Intermuscular interaction between synergists in rat originates from both intermuscular and extramuscular myofascial force transmission. Cells Tissues Organs 181(1):38–50

Maganaris CN (2004) Imaging-based estimates of moment arm length in intact human muscle-tendons. Eur J Appl Physiol 91(2–3):130–139

Maisetti O, Hug F, Bouillard K, Nordez A (2012) Characterization of passive elastic properties of the human medial gastrocnemius muscle belly using supersonic shear imaging. J Biomech 45(6):978–984

McNair PJ, Dombroski EW, Hewson DJ, Stanley SN (2001) Stretching at the ankle joint: viscoelastic responses to holds and continuous passive motion. Med Sci Sports Exerc 33(3):354–358

Meijer HJ, Rijkelijkhuizen JM, Huijing PA (2007) Myofascial force transmission between antagonistic rat lower limb muscles: effects of single muscle or muscle group lengthening. J Electromyogr Kinesiol 17(6):698–707

Nordez A, Hug F (2010) Muscle shear elastic modulus measured using supersonic shear imaging is highly related to muscle activity level. J Appl Physiol (1985) 108(5):1389–1394

Nordez A, Foure A, Dombroski EW, Mariot JP, Cornu C, McNair PJ (2010) Improvements to Hoang et al.'s method for measuring passive length-tension properties of human gastrocnemius muscle in vivo. J Biomech 43(2):379–382

Pamuk U, Karakuzu A, Ozturk C, Acar B, Yucesoy CA (2016) Combined magnetic resonance and diffusion tensor imaging analyses provide a powerful tool for in vivo assessment of deformation along human muscle fibers. J Mech Behav Biomed Mat 63:207–219

Rijkelijkhuizen JM, Meijer HJ, Baan GC, Huijing PA (2007) Myofascial force transmission also occurs between antagonistic muscles located within opposite compartments of the rat lower hind limb. J Electromyogr Kinesiol 17(6):690–697

Standring S (2016) Gray's anatomy: the anatomical basis of clinical practice. 41st edn. Elsevier Limited, New York

Stecco C, Hammer WI (2015) Functional atlas of the human fascial system. Elsevier Ltd., Edinburgh

Street SF (1983) Lateral transmission of tension in frog myofibers: a myofibrillar network and transverse cytoskeletal connections are possible transmitters. J Cell Physiol 114(3):346–364

Tian M, Herbert RD, Hoang P, Gandevia SC, Bilston LE (2012) Myofascial force transmission between the human soleus and gastrocnemius muscles during passive knee motion. J Appl Physiol (1985) 113(4):517–523

Tijs C, van Dieen JH, Maas H (2015) No functionally relevant mechanical effects of epimuscular myofascial connections between rat ankle plantar flexors. J Exp Biol 218(Pt 18):2935–2941

Tijs C, van Dieen JH, Baan GC, Maas H (2016a) Synergistic co-activation increases the extent of mechanical interaction between rat ankle plantar-flexors. Front Physiol 7:414

Tijs C, van Dieen JH, Maas H (2016b) Limited mechanical effects of intermuscular myofascial connections within the intact rat anterior crural compartment. J Biomech 49(13):2953–2959

Yaman A, Ozturk C, Huijing PA, Yucesoy CA (2013) Magnetic resonance imaging assessment of mechanical interactions between human lower leg muscles in vivo. J Biomech Eng 135(9):91003

Yucesoy CA (2010) Epimuscular myofascial force transmission implies novel principles for muscular mechanics. Exerc Sport Sci Rev 38:128–134

Yucesoy CA, Maas H, Koopman BH, Grootenboer HJ, Huijing PA (2006) Mechanisms causing effects of muscle position on proximo-distal muscle force differences in extra-muscular myofascial force transmission. Med Eng Phys 28(3):214–226

Yucesoy CA, Koopman BH, Grootenboer HJ, Huijing PA (2008) Extramuscular myofascial force transmission alters substantially the acute effects of surgical aponeurotomy: assessment by finite element modeling. Biomech Model Mechanobiol 7(3):175–189

Zajac FE (1989) Muscle and tendon: properties, models, scalin, and application to biomechanics and motor control. Crit Rev Biomed Eng 17(4):359–411